Environmental Research 205 (2022) 112469

Contents lists available at ScienceDirect

Environmental Research

journal homepage: www.elsevier.com/locate/envres

Spatial distribution and origin of organic matters in an Arctic fjord system based on lipid biomarkers (*n*-alkanes and sterols)

Jong-Ku Gal [a], Bo Kyung Kim [a], Hyoung Min Joo [a], Chorom Shim [a], Boyeon Lee [a], Il-Nam Kim [b], Jinyoung Jung [a], Kyung-Hoon Shin [c], Sun-Yong Ha [a,*]

[a] Division of Ocean Sciences, Korea Polar Research Institute, 26 Songdomirae-ro, Incheon, South Korea
[b] Department of Marine Science, Incheon National University, 119 Academy-ro, Incheon, South Korea
[c] Department of Marine Sciences and Convergence Technology, Hanyang University, 55 Hanyangdeahak-ro, Ansan, South Korea

ARTICLE INFO

Keywords:
N-alkanes
Sterols
Lipid biomarkers
Tidewater glacier
Kongsfjorden

ABSTRACT

The concentration of n-alkanes (C_{17}–C_{35}) and sterols in marine particulate matter were investigated to trace the origin of organic carbon in Kongsfjorden in early spring (April). The spatial distributions of environmental factors (seawater temperature, salinity, density, turbidity, chlorophyll *a* (chl. *a*) and particulate organic carbon (POC) concentrations) and the cell density of phytoplankton differed between the inner and outer fjord regions. In addition, brassicasterol, diatom biomarker, showed a high concentration in the outer fjord and positive correlations with the chl. *a* and POC concentrations in the water column. In contrast, some sterols originating from terrestrial organic matter (OM), such as stigmasterol and campesterol, showed relatively higher concentrations in the inner fjord than in the outer fjord. Based on the distance-based redundancy analysis (db-RDA) result, the distributions of organic compounds are predominantly controlled by the water density and the POC and chl. *a* concentrations, and these distributions allowed us to divide the inner and outer fjord regions. However, the hierarchical clustering of principal components (HCPC) results obtained based on principal component analysis (PCA) using lipid biomarkers (C_{17}–C_{35} alkanes and sterols) and environmental factors indicated that the clusters were distinguished by surface (0 m) and subsurface (>4 m) seawater samples rather than by any regional division. Notably, the concentration of relatively short-chain alkanes (average chain length (ACL): 24.6 ± 3.7) without a carbon preference for odd numbers (carbon preference index (CPI): 0.97 ± 0.11) in the sea surface layer was significantly higher than that of subsurface seawater (ACL: 31.1 ± 0.5 and CPI: 1.06 ± 0.03) in the early spring. This suggests the potential of these compounds as indicators for tidewater glacier-derived OM and freshwater input by snow melt into the fjord system. Hence, these results demonstrate that the distributions of lipid biomarkers in the water column possibly provide important information for a comprehensive understanding of the origin and transport of OM in an Arctic fjord.

1. Introduction

The retreat of tidewater glaciers has been observed in the Arctic and Antarctic fjord systems over the past decades (Moon et al., 2015; Schellenberger et al., 2015; Vieli et al., 2002). According to climate prediction models, the effects of climate warming could involve the release of large amounts of stored water via the removal or melting of Arctic permafrost, snow and glaciers (Syvitski et al., 1998, 2003; Box et al., 2019; Randers and Goluke, 2020). In particular, fjord systems which end from the glacier to the sea are susceptible to climate change. The increases in meltwater outflow resulting from tidewater glacier retreat lead to changes in sea temperature, salinity, and freshwater runoff and also support terrestrial OM in the marine environment (Hopwood et al., 2020; McGovern et al., 2020).

Previous studies have suggested the potential effect of labile dissolved organic carbon (DOC) derived from glaciers on marine food webs via microbial activity (Han et al., 2020; Hood et al., 2009; Smith et al., 2017). In contrast, POC is mainly deposited in front of glaciers, and the labile proportion of POC is relatively less than that of DOC, but glacier-derived POC fluxes into the marine environment were found to be larger than those of DOC (Lawson et al., 2014). The dynamics of glaciers in polar regions are the dominant processes that transport

* Corresponding author.
E-mail address: syha@kopri.re.kr (S.-Y. Ha).

https://doi.org/10.1016/j.envres.2021.112469
Received 5 April 2021; Received in revised form 9 November 2021; Accepted 24 November 2021
Available online 1 December 2021

particles into the sediments (Alley et al., 1997; Stein et al., 1994). Therefore, the recently observed rapid retreat of Arctic glaciers makes POC an important factor in the carbon budget changes of fjord systems. Nevertheless, evaluations of the biogeochemical effects of glacial-derived POC inputs into the marine environment are insufficient because it is difficult to identify and assess the origin of freshwater entering a marine environment. Consequently, understanding the composition and cycle of POC in fjord systems derived from glaciers could be a key factor in understanding global climate change and the carbon cycle.

Lipid biomarkers, such as *n*-alkanes and sterols, are useful indicator to provide evidence for the distribution and origin of OMs in marine environments. Especially, *n*-alkanes are produced by terrestrial plants, aquatic plants and algae. In general, short-chain alkanes are originated from algae and bacteria, whereas long-chain alkanes are originated from terrestrial plants representing a higher value of average chain length (ACL; Cranwell et al., 1987; Poynter and Eglinton, 1990). Carbon preference index (CPI) is calculated by the relative abundances of odd-to-even number *n*-alkanes in a certain carbon number range (Bray and Evans, 1961; Matsuda and Koyama, 1977; Marzi et al., 1993). In the distribution of alkane, the odd carbon preference for even number is different depending on the producer. For instance, terrestrial higher plants have a typical value of CPI (>5), whereas CPI of petrogenic alkanes shows no carbon preference, close to 1, with a smooth distribution (Eglinton and Hamilton, 1967; Bush and McInerney, 2013). Therefore, ACL and CPI provide valuable information on *n*-alkane sources.

Sterols are also useful molecular biomarkers to identify the origin of OMs. Brassicasterol and dinosterol are known as phytosterols produced by marine diatoms and dinoflagellate, respectively (Boon et al., 1979; Volkman, 1986). Moreover, campesterol, stigmasterol, and β-sitosterol, which are predominantly contained in terrestrial plants, have been used as indicators of terrestrial OM (Huang and Meinschein, 1976; Volkman, 1986). Therefore, *n*-alkanes and sterols are suitable tracers of OM in the Arctic environments, which includes mixtures of OM from the glacier, snow, terrestrial and marine environments (e.g. Yunker et al., 1995; Kim et al., 2011; Rontani et al., 2018).

The Kongsfjorden system, a high-latitude Arctic fjord, is a very suitable experimental place for organic material circulation research involving glacial melting because active changes in the marine environment can be observed in this region depending on the season. The seasonal variations in Kongsfjorden introduce an ideal natural laboratory that can serve as a biogeochemical and functional indicator of climate change. There are five tidewater glaciers in the inner fjord that mainly support the input of freshwater into the fjord by seasonal glacial melting starting in early spring (April) (Pramanik et al., 2018). The estimated mean annual glacial POC input into Kongsfjorden is approximately 760 tons per year according to the mean freshwater volume and POC concentration measured in the water column (Kuliński et al., 2014). In the Arctic early spring, large quantities of OM begin to enter the fjord system; these inputs can lead to massive turbid water in the inner fjord, limiting the light in the water column and possibly decreasing the production of phytoplankton (Hopwood et al., 2020). However, few studies have been conducted on the distributions of organic compounds or their origins using *in situ* seawater samples in high Arctic fjord systems due to the difficult access to field sites being hampered by floating ice and fragmented glaciers in early spring (e.g. Brogi et al., 2019; McGovern et al., 2020).

In the present study, we investigated (1) spatial variations in lipid biomarkers, such as *n*-alkanes and sterols, to identify the origin of OM using seawater samples from the Kongsfjorden in early spring (April). Furthermore, (2) we tested the potential of lipid biomarkers as an indicator of glacier-derived and/or terrestrial OMs in an Arctic fjord system by comparing them with phytoplankton cell density and environmental factors (seawater temperature, salinity, density, turbidity, chl. *a* and POC concentrations).

2. Materials and methods

2.1. Sample collection

Sample collection was conducted at 8 stations onboard the R/V Teisten in early spring (April 2018) when the tidewater glaciers started to melt at Kongsfjorden, Svalbard (Fig. 1). During this period, a large number of large glaciers floated on the water surface, and adverse weather conditions allowed the collection of seawater samples only over a limited timeframe. Moreover, we have to use all of seawater samples for a single injection for chemical analysis, such as POC, chl. *a*, and lipid biomarkers, due to the low concentration in the seawater samples. Therefore, only a single dataset could be obtained for this study.

A conductivity-temperature-depth (CTD) system (RBR concerto 3) was used to obtain the water temperature, salinity, turbidity, and density measurements. Here, temperature and salinity data were published in Choi et al. (2020), wherein the data were obtained by the same CTD logger system in this study.

To determine sample collection, density gradient and autochthonous sources, especially terrestrial sources, were considered for comparison with water mass, which major control factor in the ambient environmental setting, and phytoplankton cell density. Onboard observation using the CTD logger system showed significant temperature and salinity gradient from surface to 10 m water depth (Fig. 2). Therefore, the collection of seawater samples was concentrated from the surface to euphotic depth, and bottom water (10−20 m above the bottom). The seawater samples were collected using a Niskin water sampler according to the light penetration depth estimated by a Secchi disk using the vertical attenuation coefficient (Kd = 1.7/Secchi depth) as described by Kim et al. (2020). Seawater samples were collected at depths up to 100 m at 100, 30 and 5% light intensities compared to that of the surface seawater (100%) (Table 1). To identify phytoplankton species, 100-mL seawater samples were collected at each water depth and stored in 125-mL bottles preserved with glutaraldehyde (at a final concentration of 1%). The samples that had been fixed by glutaraldehyde were filtered by Gelman GN-6 Metricel filters (pore size of 0.45 μm; Gelman Sciences, USA).

The seawater samples were filtered by a precombusted glass fiber filter (GF/F, pore size of 0.7 μm, Whatman, UK) to analyze the POC, chlorophyll *a* (chl. *a*), sterol and *n*-alkane concentrations. The filter samples used for the POC, sterol and *n*-alkane analyses were immediately stored at −20 °C, freeze-dried and moved to the laboratory. The filters used for the chl. *a* analysis were immediately stored at −80 °C until the analysis was conducted.

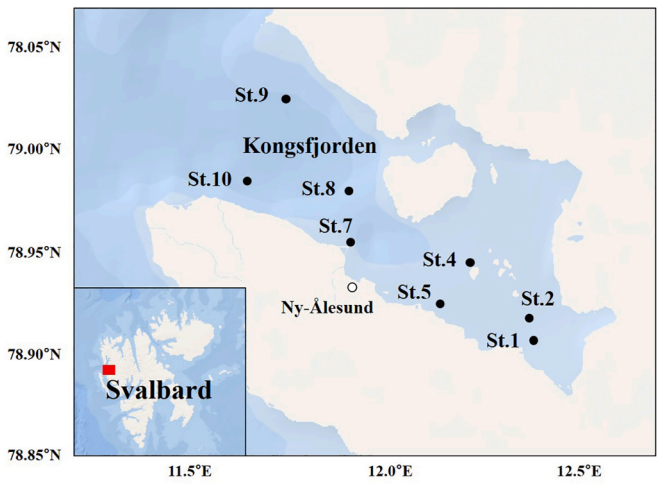

Fig. 1. Map of the study area in Kongsfjorden, Svalbard.

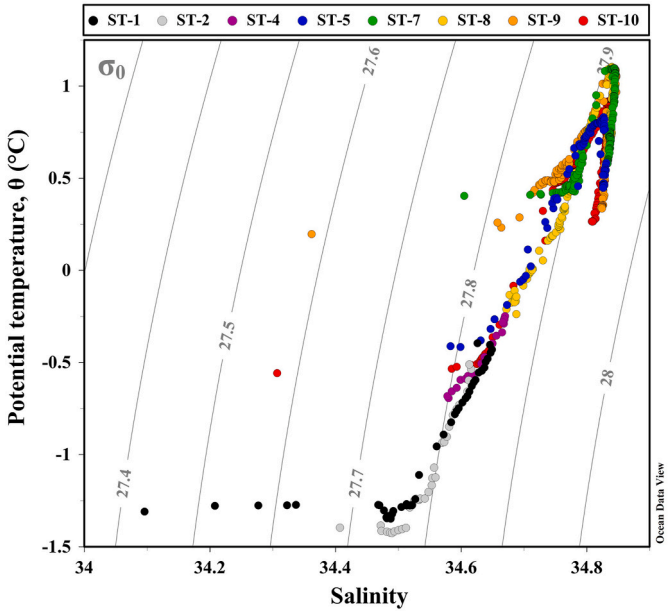

Fig. 2. T-S diagram in the study area.

2.2. POC, chl. a and phytoplankton species

The samples used to determine the POC concentrations were acidified by HCl fuming overnight in a desiccator to remove inorganic carbon, as described by Jung et al. (2020). After acidification, the samples were neutralized using NaOH pellets and silica gel was placed in a desiccator with samples and was kept in vacuum. The samples were then enveloped in a tin capsule, and the POC concentrations were measured with an elemental analyzer (vario MACRO cube, Elementar, Germany). The analytical precision (1 σ; standard deviation) was obtained by running the standard (acetanilide), and the precision was ±4%.

The filter samples used for the chl. *a* analyses were extracted using 90% acetone at 4 °C for 12 h within 24 h after sample collection (Parsons et al., 1984). The chl. *a* concentrations were determined using a Trilogy fluorometer (Tuner Designs, USA). The fluorometer calibration was performed with a liquid primary chl. *a* standard (Turner designs, USA).

The phytoplankton pretreatment, identification and counting details are described in Kim et al. (2020). Briefly, a filter was mounted on a microscope slide in an aqueous embedding medium (2-hydroxypropyl methacrylate, HPMA). Phytoplankton was identified from HPMA slides with an optical microscope (BX53TR-32FB3F0 microscope, Olympus, Inc., Tokyo, Japan). The genera identification and cell counts were conducted as described by Kang et al. (1993), Round and Mann (1990) and Tomas (1997).

2.3. Lipid extraction and analysis

Internal standards (squalane and 5-α-androstan-3β-ol (Sigma-Aldrich, USA)) were added to the freeze-dried samples prior to lipid extraction. The samples were extracted by sonication with dichloromethane:methanol (2:1, v:v) according to the method described by Gal et al. (2018b). The total lipid extracts were separated into two fractions over a SiO_2 column. The apolar and polar fractions were eluted using hexane and dichloromethane:methanol (1:1 v:v), respectively. The polar fraction was silylated with N,O-bis(trimethylsilyl)trifluoroacetamide

Table 1
Concentrations of n-alkanes and carbon preference index (CPI) and average chain length (ACL) values. The hierarchical clustering of principal component (HCPC) clusters indicates the detailed values shown in Fig. 5B. Groups were defined in consideration of the results of principal component analysis (PCA) and nonmetric multidimensional scaling (NMDS) shown in Fig. 4.

Site	Depth	Total n-alkanes	Sum [C19–C21]	Sum [C27–C29]	Sum [C31–C33]	CPI	ACL	HCPC cluster	Group
	[m]	[ng/L]	[ng/L]	[ng/L]	[ng/L]				
St.1	0	44	27	0	0	1.12	21.0	1	IN
St.1	10	1208	16	214	550	1.06	31.0	2	IN
St.1	30	1685	0	341	764	1.04	31.4	2	IN
St.1	50	900	0	168	403	1.06	31.4	2	IN
St.2	0	81	0	15	24	0.90	31.5	3	IN
St.2	4	458	0	93	207	1.05	31.3	2	IN
St.2	9	882	0	145	404	1.05	31.3	2	IN
St.2	35	827	0	137	383	1.08	31.3	2	IN
St.4	0	90	42	0	0	0.84	21.9	1	IN
St.4	5	97	0	21	41	1.11	31.1	2	IN
St.4	10	346	0	64	152	1.04	31.1	2	IN
St.5	0	1375	584	102	47	0.88	23.7	1	IN
St.5	5	965	0	176	447	1.04	31.6	2	IN
St.5	12	295	0	54	130	1.04	31.1	2	IN
St.5	80	195	0	39	88	1.06	31.5	2	IN
St.7	0	160	77	0	0	0.89	23.6	1	OUT
St.7	7	278	0	46	137	1.09	31.4	2	OUT
St.7	18	718	0	128	323	1.04	31.5	2	OUT
St.7	80	201	0	37	85	1.03	30.8	2	OUT
St.8	0	272	153	0	0	1.11	21.0	1	OUT
St.8	10	103	0	21	44	1.04	31.1	2	OUT
St.8	40	116	0	20	49	1.03	31.2	2	OUT
St.8	100	151	0	28	71	1.08	31.2	2	OUT
St.9	0	285	35	82	43	1.01	27.1	3	OUT
St.9	10	81	0	19	31	1.05	30.5	2	OUT
St.9	30	234	0	46	104	1.06	31.2	2	OUT
St.9	50	261	0	51	118	1.07	31.3	2	OUT
St.9	100	210	0	36	96	1.08	31.2	2	OUT
St.10	0	673	59	211	107	0.98	27.2	3	OUT
St.10	5	1157	0	226	457	1.00	30.7	2	OUT
St.10	12	541	0	103	242	1.05	31.2	2	OUT
St.10	50	176	5	34	56	1.12	29.4	2	OUT
St.10	100	168	0	43	65	1.02	30.2	2	OUT

(BSTFA) and heated at 70 °C for 1 h.

The sterols in the polar fraction and n-alkanes in the apolar fraction were analyzed using an Agilent 5977 E GC/MSD (Agilent Technologies, Santa Clara, CA) with an HP-5 column (30 m × 0.25 mm, 0.25 μm, Agilent). The oven temperature was programmed to change from 40 °C to 300 °C at a rate of 10 °C/min and maintained at 300 °C for 10 min. The electron ionization energy was 70 eV, and helium was used as a carrier gas (1 mL/min). Scanning was performed in full-scan mode (m/z 50–650) and in the selected ion monitoring (SIM) modes of *m/z* 99 (n-alkanes), *m/z* 333 (5-α-androstan-3β-ol), *m/z* 370 (coprostanol and epicoprostanol), *m/z* 382 (stigmasterol), *m/z* 396 (β-sitosterol), *m/z* 484 (stigmasterol), *m/z* 458 (cholesterol) and *m/z* 470 (Brassicasterol).

Individual *n*-alkane compounds (C_{17}–C_{35}) were identified based on a comparison of the relative retention times of analytical standards (Supelco 502,065, AccuStandard, USA) (Kim et al., 2017). The identification of sterols was conducted based on the retention times and mass spectra of the analytical standards (Sigma-Aldrich, USA). The quantification of individual compounds was performed based on the relative response factors of standard compounds compared with those of internal standards (squalane for *n*-alkanes, 5α-androstan-3β-ol for sterols). The limit of detection was calculated as 3 times the signal to noise ratio and the limit of quantification applied 10 times the signal to noise ratio (ca. 80 pg alkane and 20 pg sterol). The precision of the sterol and *n*-alkane analyses was obtained by an in-house reference standard (Gal et al., 2018a), and the precisions for each compound and relative standard deviation (RSD) are displayed in Table 2 and S3. RSD was calculated as follows:

$$\mathrm{RSD} = 100 \times \frac{s}{\bar{x}}$$

where s is the standard deviation of the in-house reference standard. $\bar{x}$ is the mean value of concentration of the in-house reference standard.

The ACL (Cranwell et al., 1987; Poynter and Eglinton, 1990) and CPI (modified from Bray and Evans, 1961) were calculated on the entire carbon range as follows:

$$\mathrm{ACL} = \frac{\sum (\mathrm{n} \times \mathrm{Cn}) 17 - 35}{\sum (\mathrm{C17} - 35)}$$

$$\mathrm{CPI} = \frac{1}{2} \times \left[\left(\frac{\sum \mathrm{odd}\ \ \mathrm{C17} - 33}{\sum \mathrm{even}\ \ \mathrm{C18} - 34} \right) + \left(\frac{\sum \mathrm{odd}\ \ \mathrm{C19} - 35}{\sum \mathrm{even}\ \ \mathrm{C18} - 34} \right) \right]$$

where Cn is the concentration of the n-alkane containing n carbon atoms.

2.4. Statistics and data analysis

To determine the presence of general relationships among the spatial distributions of phytoplankton species, lipid compounds (sterols and *n*-alkanes) and environmental parameters (temperature, salinity, turbidity, density, and POC and chl. a concentration), principal component analysis (PCA) was performed using the R program (R Development Core Team, 2015). We also performed hierarchical clustering of principal components (HCPC) on the PCA results using the R program. A distance-based redundancy analysis (db-RDA) was performed to identify the major component of the spatial distribution of lipid compounds in the water column. Nonmetric multidimensional scaling (NMDS) was performed to identify the differences between inner and outer fjords based on the phytoplankton cell density and environmental factors using the R program. PCA and RDA were performed on the fractional abundances of sterols and *n*-alkanes, which were obtained by normalizing each sterol and *n*-alkane concentration to the summed concentration of all of the sterols and *n*-alkanes considered in this study, respectively. The statistical analyses (two sample *t*-test) of the differences in data between the inner and outer fjord regions and among different depths were performed using the R program.

3. Results

3.1. Environmental conditions

The potential temperature (θ) and salinity in Kongsfjorden ranged from −1.4–1.1 °C and 34.1–34.8, respectively (Fig. 2). The vertical profiles of temperature and salinity indicate low temperatures and a weak pycnocline in this season (Choi et al., 2020). However, according to the T-S diagram, the thin upper layers (up to 5 m) were slightly colder and fresher than other layers (Fig. 2). In particular, the temperatures and salinities measured at sites 1 and 2 were lower than those measured at the other sites. The density of the surface seawater ranged from 27.58 to 27.72 kg/m^3 (27.72 ± 0.11 kg/m^3), and these density values were slightly lower than those measured at depths above 4 m, where the water densities ranged from 27.76 to 28.39 kg/m^3 (average 28.02 ± 0.20 kg/m^3) (Fig. 3A). In particular, the inner fjord sites had relatively lower measured densities due to the collapse of the tidewater glaciers in this season. The turbidity values measured at sites 1 and 2 (ranging from 1.72 to 2.90 FTU, average 2.35 ± 0.41 FTU) were relatively higher than those measured at other sites (0.32–2.94 FTU, average 1.01 ± 0.86 FTU) (*t*-test, t = 5.9379, df = 25.814, *p*-value = 2.97E−06) (Table 1).

3.2. POC, chl. a, and phytoplankton

POC concentration ranged from 0.22 to 0.31 mg/L (average 0.26 ± 0.02 mg/L) at all depths in the study area (Table S1). In most sites, the POC concentrations were highest in the surface seawater except sites 4 and 5, where have the lowest sea surface POC concentrations compared to other sites. POC concentrations in sites 4 and 5 were high at 10 m and 12 m water depth, respectively (Fig. 3B). Chl. *a* concentration ranged 0.01–0.09 mg/m^3 (average 0.04 ± 0.02 mg/m^3) at all depths in the study area. The concentration of chl. *a* showed a high value in the upper layer within 5 m of the water depth and showed a low concentration as the water depth increased (Fig. 3C). Spatial distribution of chl. *a* concentration was similar to POC (R^2 = 0.61, Fig. S1). Bacillariophyceae was dominant at all sites in the study area (Table S2). The cell density of Bacillariophyceae in the inner fjord was not significantly different from that of the outer fjord (*t*-test, t = −0.505, df = 19.628, *p*-value = 0.619). Dinophyceae and Chlorophyceae were identified in the outer fjord, however, Prymneosiophyceae was identified only in the inner fjord.

3.3. Concentrations of n-alkanes and sterols

The concentration of brassicasterol ranged 2.71–19.94 ng/L (average of 7.70 ± 3.71 ng/L) at all depths in the study area (Table 2). Similar to the chl. *a* concentrations, the brassicasterol concentrations were high in the inner fjord sites and the surface layers of the outer fjord sites (Fig. 3D). On the other hand, the concentrations of β-sitosterol and stigmasterol were high in the inner fjord sites, ranging from 2.17 to 28.95 ng/L (average 8.92 ± 7.26 ng/L) and 0.00–9.54 ng/L (average 2.89 ± 2.61 ng/L) at all depths, respectively (Fig. 3E and Table 2). Campesterol had a similar distribution to β-sitosterol, with slightly higher concentrations measured in the middle depths (approximately 30–50 m) of the euphotic zone (Fig. 3F). The correlation coefficient between the concentrations of brassicasterol and chl. *a* was (R^2 = 0.64) higher than that between the brassicasterol and POC concentrations (R^2 = 0.32) (Fig. S1). The correlation coefficient value between stigmasterol and β-sitosterol was 0.98, indicating that these compounds have the same source in the study area (Fig. S1).

Long-chain alkanes (>C_{27}) showed higher concentrations in the inner fjord than in the outer fjord (Fig. 3G and H). However, unlike the chl. *a* concentrations, the long-chain alkane concentrations were slightly higher at sites 5–8 and subsurface depths (5–30 m). Interestingly, short-chain alkanes (<C_{23}) showed a distinctly high concentration in the surface layer (Fig. 3I). The sum of the C_{19}–C_{21} concentrations ranged from 0.00 to 584.42 ng/L (average 112.23 ± 192.20 ng/L) and from

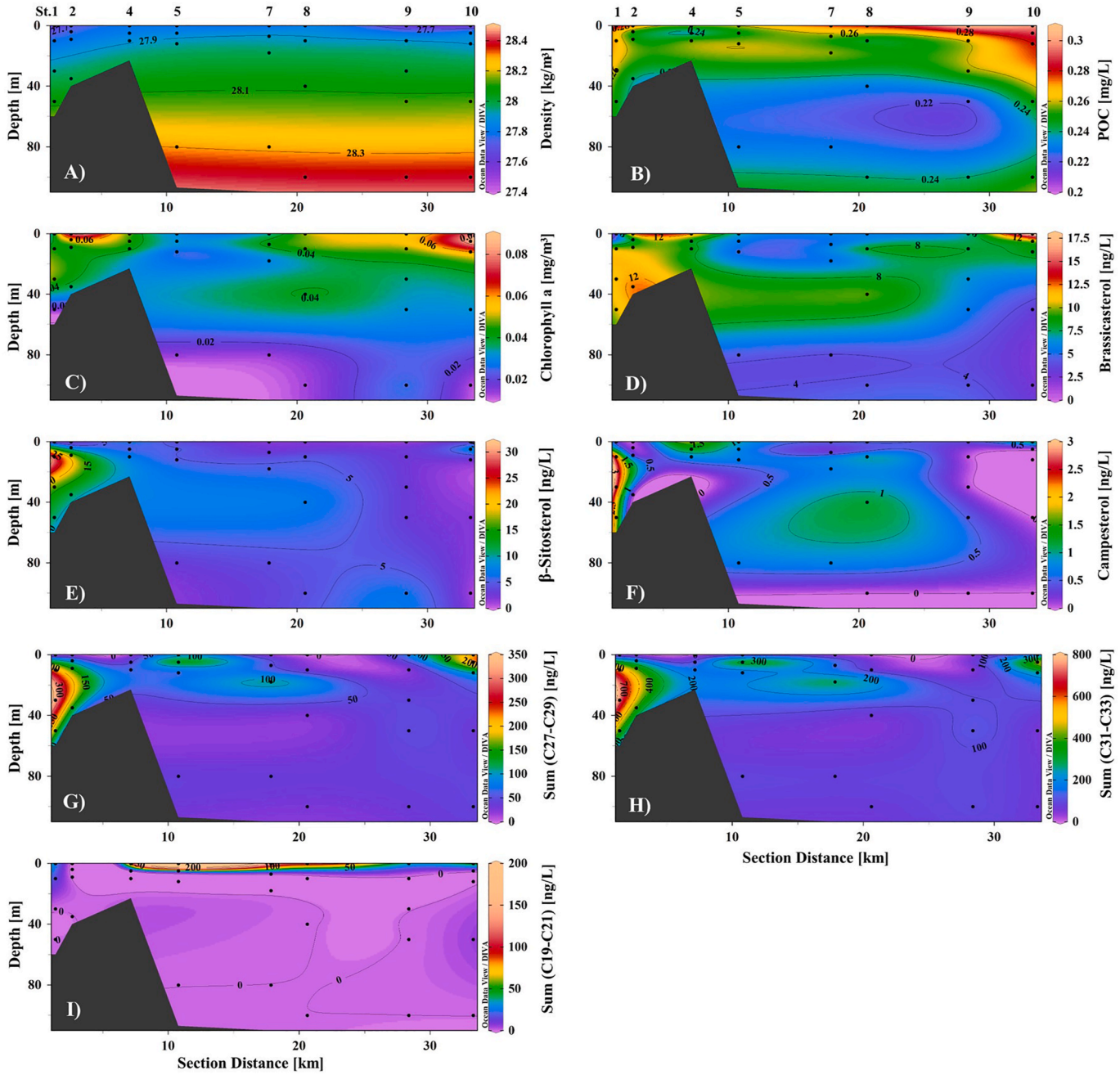

Fig. 3. Cross-section along with the inner–outer stations in Kongsfjorden: density (A), POC concentration (B), chlorophyll *a* concentration (C), brassicasterol (D), β-sitosterol (E), campesterol (F), and sum of alkanes (C_{27}–C_{29} (G), C_{31}–C_{33} (H), and C_{19}–C_{21} (I)). The group of n-alkanes was selected according to the hierarchical clustering of principal components on the principal component analysis (see Table S3).

0.00 to 15.90 ng/L (average 0.85 ± 3.31 ng/L) in the surface seawater and below the surface (>4 m), respectively (see Table S3). Statistically, the sum of the C_{19}–C_{21} concentrations was significantly higher in the surface seawater than in the subsurface seawater (*t*-test, t = 1.786, df = 7, *p*-value = 0.117).

3.4. PCA and HCPC results

The PCA results indicated that POC, chl. *a*, and cell density of Dictyochophyceae and Bacillariophyceae (the dominant species in the study area) were positively loaded on PC1, explaining 41.41% of the variance (Fig. 4A). Prymneosiophyceae and turbidity were negatively loaded on PC2, explaining 16.19% of the variance. Sites close to the ice wall (sites 1–5) were negatively loaded on PC2, while sites (sites 7–10) far from the ice wall were positively loaded on PC2. Moreover, the HCPC results showed that sites close to the ice wall belonged to Cluster 1, which is associated with relatively low water densities, high turbidities and high Prymneosiophyceae cell density. Most sites far from the ice wall belonged to Clusters 2 and 3, which are associated with relatively high densities, high POC and chl. *a* concentrations and high cell density of Bacillariophyceae (Fig. 4A and Table S2).

POC, chl. *a* and brassicasterol were positively loaded on PC2, explaining 13.82% of the variance, while stigmasterol and β-sitosterol showed negative loading on PC2 (Fig. 5A). The β-sitosterol, campesterol, and stigmasterol concentrations were negatively loaded on PC2. The C_{17}–C_{25} alkanes showed strong positive loading on PC1, explaining 42.01% of the variance. In contrast, long-chain alkanes (>C_{26}) were negatively loaded on PC1. Notably, the C_{29}–C_{33} alkanes showed strong

Table 2
Concentrations of individual sterols and analytical precision of each compound from the in-house reference (cf. Gal et al., 2018a).

Site	Depth	Coprostanol	Cholesterol	Cholestanol	Brassicasterol	Campesterol	Stigmasterol	β-Sitosterol	Total sterols	HCPC cluster	Group
	[m]	[ng/L]	[ng/L]	[ng/L]	[ng/L]	[ng/L]	[ng/L]	[ng/L]	[ng/L]		
St.1	0	LOD	6.9	1.3	3.6	0.4	0.6	2.2	14.9	1	IN
St.1	10	4.4	12.1	1.3	10.6	2.6	9.5	29.0	69.4	2	IN
St.1	30	12.7	13.3	1.6	11.1	2.8	6.6	16.2	64.3	2	IN
St.1	50	0.7	15.0	2.8	10.5	1.8	2.8	11.0	44.7	2	IN
St.2	0	9.2	15.1	LOD	13.5	LOD	LOD	3.1	41.0	3	IN
St.2	4	0.3	7.9	1.0	7.3	LOD	2.3	6.0	24.6	2	IN
St.2	9	1.2	10.9	2.4	9.5	LOD	5.9	17.6	47.4	2	IN
St.2	35	1.0	24.6	3.7	12.6	LOD	4.3	11.6	57.9	2	IN
St.4	0	LOD	21.2	3.1	13.0	1.9	1.4	7.4	48.1	1	IN
St.4	5	0.2	21.6	1.9	8.2	1.5	1.6	4.7	39.7	2	IN
St.4	10	LOD	12.9	2.1	9.6	0.9	2.0	7.2	34.7	2	IN
St.5	0	0.3	42.7	3.1	6.1	0.8	1.0	3.9	57.9	1	IN
St.5	5	0.2	12.8	1.5	5.4	0.7	2.2	6.0	28.8	2	IN
St.5	12	0.4	12.6	1.7	4.2	0.7	1.8	4.8	26.2	2	IN
St.5	80	0.3	7.4	1.3	4.5	0.7	1.2	3.2	18.5	2	IN
St.7	0	0.1	7.3	1.6	6.3	0.5	0.6	1.5	17.9	1	OUT
St.7	7	0.4	7.2	1.1	5.0	LOD	LOD	2.0	15.5	2	OUT
St.7	18	0.1	8.1	0.9	4.9	0.7	1.7	5.3	21.7	2	OUT
St.7	80	0.3	8.6	1.0	3.7	0.7	1.3	4.2	19.9	2	OUT
St.8	0	LOD	7.4	1.3	5.6	0.6	0.8	2.4	18.1	1	OUT
St.8	10	0.3	16.4	3.1	9.3	1.3	1.5	5.5	37.3	2	OUT
St.8	40	0.5	12.6	1.7	9.9	1.2	2.0	7.2	35.2	2	OUT
St.8	100	0.5	4.9	1.5	4.4	LOD	1.5	4.2	17.0	2	OUT
St.9	0	LOD	5.0	1.2	6.8	0.4	0.2	1.1	14.7	3	OUT
St.9	10	0.2	5.8	1.3	8.1	LOD	0.9	2.6	18.8	2	OUT
St.9	30	LOD	5.3	1.0	6.3	LOD	0.8	2.9	16.3	2	OUT
St.9	50	LOD	5.6	0.7	5.5	0.5	0.8	2.8	15.8	2	OUT
St.9	100	0.5	4.8	1.3	4.2	LOD	2.2	6.6	19.6	2	OUT
St.10	0	LOD	18.0	2.0	19.9	1.3	LOD	2.6	43.9	3	OUT
St.10	5	LOD	5.3	0.7	9.4	LOD	2.4	7.8	25.5	2	OUT
St.10	12	0.2	4.7	0.6	8.8	LOD	0.7	2.4	17.3	2	OUT
St.10	50	0.3	3.7	0.6	3.5	LOD	0.8	2.0	10.9	2	OUT
St.10	100	0.5	13.9	0.3	2.7	LOD	LOD	1.1	18.6	2	OUT
In-house[a]	Avr (ng/g)	32.3	173.4	163.1	223.2	252.9	89.8	307.8			
	STD (±1 σ)	4.1	35.9	23.1	44.4	43.7	27.7	55.9			
	%RSD	13	21	14	20	17	31	18			

[a] In-house reference sediment (cf. Gal et al., 2018a), LOD: below limit of detection (ca. 20 pg sterol).

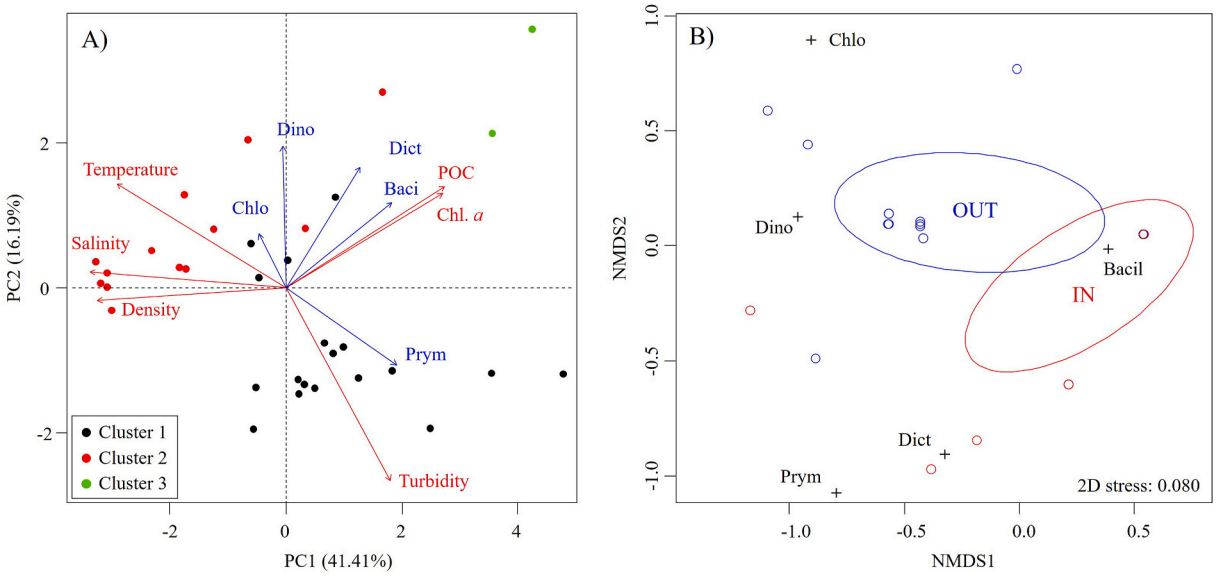

Fig. 4. Biplot of the results of principal component analysis (PCA) and hierarchical clustering of principal components (HCPC) of the fractional abundances of phytoplankton and environmental parameters (A). Nonmetric multidimensional scaling (NMDS) result showing the groups of inner and outer fjord sites considering the PCA and HCPC results (B). POC: Particulate Organic Carbon, Chl. *a*: chlorophyll *a*, Dino: Dinophyceae, Baci: Bacillariophyceae, Dict: Dictyochophyceae, Chlo: Chlorophyceae, Prym: Prymneosiophyceae.

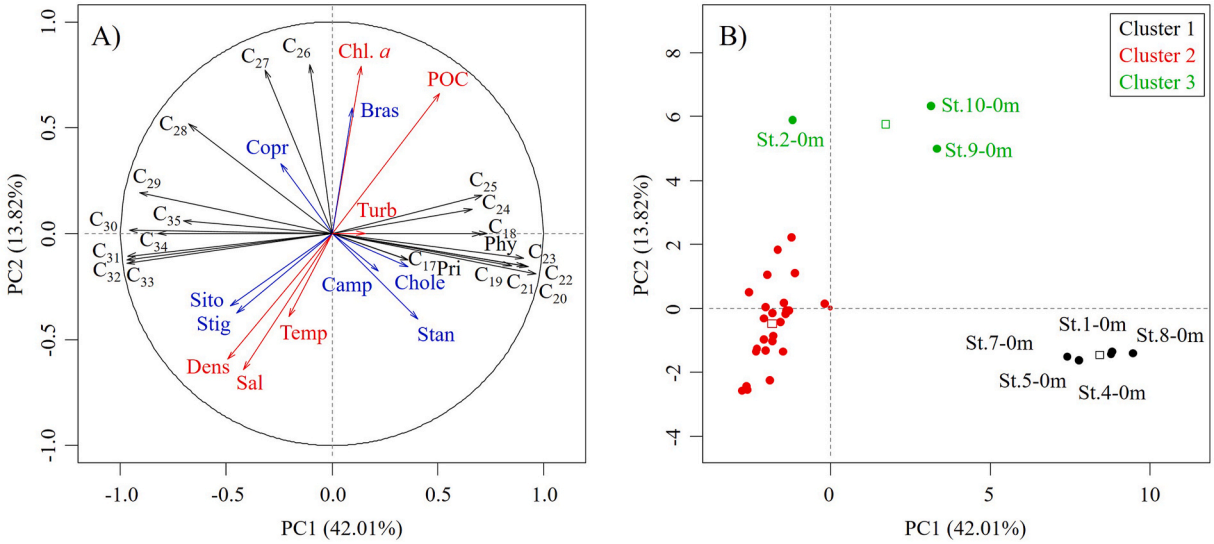

Fig. 5. Results of the principal component analysis (PCA) (A) and hierarchical clustering of principal components (HCPC) (B) of the fractional abundances of *n*-alkanes (black lines), sterols (blue lines) and environmental parameters (red lines). The detailed clustering results are shown in Table 1 and S2. Chl. *a*: Chlorophyll *a*, POC: Particulate Organic Carbon, Temp: Temperature, Sal: Salinity, Dens: Density, Turb: Turbidity, Bras: brassicasterol, Copr: Coprostanol, Chole: Cholesterol, Stan: Cholestanol, Camp: Campesterol, Sito: β-sitosterol, Stig: Stigmasterol. (For interpretation of the references to colour in this figure legend, the reader is referred to the Web version of this article.)

negative loading on PC 1.

Three clusters were distinguished by HCPC based on the PCA results (Fig. 5B). Notably, clusters 1 and 3 consist only of surface seawater samples in the study area. Clusters 1 and 3 had significantly lower concentrations of stigmasterol (t = −3.6004, df = 29.592, *p*-value = 0.00057) and β-sitosterol (t = −2.7668, df = 30.968, *p*-value = 0.00473) than that of cluster 2; additionally, clusters 1 and 3 had higher sums of C_{31}–C_{33} alkanes than that of cluster 2 (t = −4.6135, df = 28.604, *p*-value = 3.82E-05). In contrast, the sums of C_{19}–C_{21} alkanes of clusters 1 and 3 were higher than that of cluster 2 (t = 1.7862, df = 7.0013, *p*-value = 0.0586).

4. Discussion

4.1. Zonation of phytoplankton distribution

The cell density of phytoplankton and primary production in the inner fjord sites were lower than those of the outer fjord sites due to light inhibition and nutrient availability attributed to glacial melting (Halbach et al., 2019; Kim et al., 2020). According to the HCPC results of the environmental conditions and phytoplankton cell density, we defined the inner (sites 1–5) and outer fjord (sites 7–10) regions in this study (Fig. 4A and Table 2). The NMDS results also showed a distinction between the inner and outer fjord sites, which were defined based on the cluster results (2D stress = 0.080, Fig. 4B). This zonation is consistent with the separation between the inner and outer fjords obtained by the regional distribution of zooplankton collected during the same period (Choi et al., 2020).

Based on the fluorescence spectroscopy analysis conducted in Kongsfjorden, the influx of labile dissolved OM due to the melting of sea ice and glaciers in early spring determines the dissolved OM properties, which showed a high total fluorescence and a high proportion of tyrosine-like compounds of approximately 58% of the total fluorescence in surface seawater (Brogi et al., 2019). On the other hand, according to the 6-year flux data in Kongsfjorden, the opal which indicate diatom production (autochthonous) and POC fluxes measured in early spring were increased compared to those measured in the winter season due to the contribution of autochthonous carbon sources (D'Angelo et al., 2018). These factors might be caused by high sedimentation rates and resuspension in front of the tidewater glaciers of Kongsfjorden (Koziorowska et al., 2017). Later, in summer, primary production is enhanced by solar radiation during the bloom period, while the opal/organic carbon ratio is decreased by the mixture of OM sources from autochthonous and terrestrial inputs (D'Angelo et al., 2018; Iversen and Seuthe, 2011). Combining the results of PCA obtained in this study with those of previous studies, as glaciers and sea ice melt in early spring, the influxes of particulate and dissolved matter increase in the inner part of Kongsfjorden. As a result, the region shows a low contribution of autochthonous sources to POC resulting from the lower primary productivity caused by the increased turbidity and light penetration in the water column. In conclusion, it appears that clusters according to the distance from the ice wall during the glacial melting period by the change of light conditions and primary production in Kongsfjorden.

4.2. Spatial distribution and origin of OM

The similar distributions and loadings on the PCA plots of the POC, chl. *a* and brassicasterol concentrations indicate that these components may have had the same factors controlling their distributions in the water column (Fig. 5A). Considering the PCA results obtained based on the cell density of phytoplankton (Fig. 4A), the controlling factor for their spatial distribution was considered to be an abundance of marine diatoms (Bacillariophyceae), which are considered to be the main producers of brassicasterol (Volkman et al., 1998). This means that the relatively high POC concentration observed in the outer fjord consisted of autochthonous OM originating from diatoms. Moreover, the regional distinctions (between the inner and outer fjord) obtained based on the distributions of phytoplankton and environmental factors imply that the distribution of autochthonous sources in the study area is determined by the distance of the measurement site from the glaciers as well as by their influences.

The clustering result of HCPC obtained based on the lipid composition data was different from that obtained using the phytoplankton cell density, which showed the clustering of the inner and outer fjord sites (Table 1). In the db-RDA result, the main factors determining the spatial distribution of the lipid compounds were the water density and the POC and chl. *a* concentrations (Fig. 6). The db-RDA results showed no difference between the inner and outer fjord sites classified as

phytoplankton-based HCPC. However, in the case of sterols, which had a weak load in PCA, a tendency to be divided into inner and outer regions was observed (see Fig. 3D–F). In particular, terrestrial sterols, such as stigmasterol, coprostanol and β-sitosterol, showed high concentrations in the inner fjord, whereas high concentrations of autochthonous compounds were found in the outer fjord (Hörner et al., 2016; Volkman, 1986; Yunker et al., 1995). Moreover, long-chain alkanes (>C_{27}) also showed a similar distribution in the water column compared to that of terrestrial sterols (Fig. 3G and H). This means that the distribution of organic compounds in the subsurface layer is controlled by primary production, which can be represented by the cell density of phytoplankton and chl. *a* in the water column. In conclusion, terrestrial OM, along with the particulate matter that increased turbidity, would have been introduced into the inner fjords along the subsurface by the collapse of tidewater glaciers and melting of sea ice (Torsvik et al., 2019). In the outer fjord where relatively high phytoplankton and chlorophyll concentrations were measured, autochthonous sources appear to be the main factors controlling the distribution of organic compounds in the water column of Kongsfjorden (Choi et al., 2020; Kim et al., 2020).

The distribution of organic compounds in each cluster is shown in Fig. 5B. In detail, short-chain alkenes dominated in cluster 1 (ACL: 22.3 ± 1.3, CPI: 0.97 ± 0.13) and cluster 3 (ACL: 28.6 ± 2.5, CPI: 0.96 ± 0.06), consisting of the surface layer (average 24.6 ± 3.7 and 0.97 ± 0.11 in ACL and CPI, respectively) (Fig. 7A and C); however, long-chain alkenes predominated in cluster 2 (ACL: 31.1 ± 0.5, CPI: 1.06 ± 0.03), which consisted of the subsurface layers (Fig. 7B). In the surface layers, it is interpreted that freshwater introduced by melting sea ice and glaciers was moving out of the fjord along the weak pycnocline, ignoring the inflow from terrestrial streams. In marine environments, short-chain alkanes are predominantly produced by aquatic algae, including phytoplankton and microorganisms, while long-chain alkanes are mostly produced by the waxes of higher plants (e.g., Brassell et al., 1978; Eglinton et al., 1962; Han and Calvin, 1969). These biogenic sources tend to be dominant with odd-carbon-number alkanes, but these sources were not found to be dominant in this study (Fig. 7). Therefore, the seawater sampled in this study showed low CPI values (see above). Petroleum and petroleum-sourced rocks can also be major alkane sources

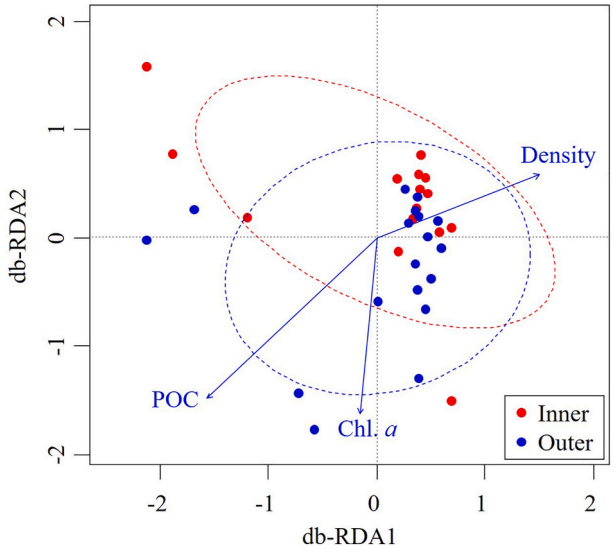

Fig. 6. Results of the distance-based redundancy analysis (db-RDA) of the fractional abundances of *n*-alkanes, sterols and environmental parameters. The red and blue dots indicate samples collected from the inner and outer sites, respectively. The red and blue circles indicate the ranges of the inner and outer sites at 90% prediction. POC: Particulate Organic Carbon, Chl. *a*: chlorophyll *a*. (For interpretation of the references to colour in this figure legend, the reader is referred to the Web version of this article.)

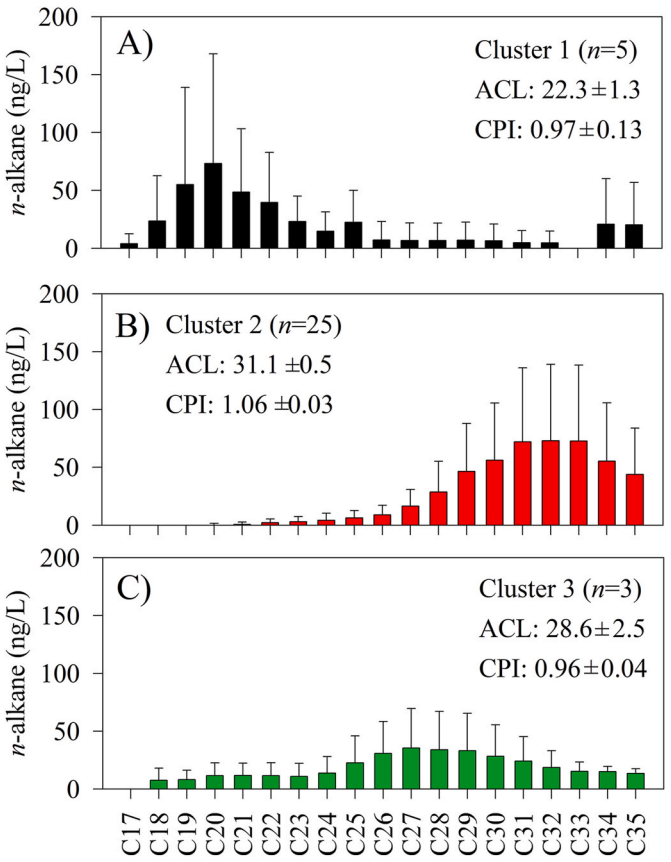

Fig. 7. Average concentrations of individual *n*-alkanes from samples of (A) cluster 1 ($n = 5$), (B) cluster 2 ($n = 25$), and (C) cluster 3 ($n = 3$) corresponding to the HCPC results shown in Fig. 5B.

(Brassell and Eglinton, 1980; Wang et al., 1999). However, the results of this study do not follow the normal pattern of petroleum-derived alkanes, which are uniformly distributed from short-to long-chain alkanes. Considering the effect of large amounts of freshwater input from glaciers in early spring, atmospheric sources via snow seem to be more reasonable than petroleum,-based sources. Additionally, this idea is consistent with the predominance of C_{18}–C_{20} alkanes obtained from aerosol samples collected in Ny Ålesund, in which no carbon preference for odd numbers of carbons was found (Cecinato et al., 2000). On the other hand, this idea contrasts with measured sea spray samples that indicated abundant C_{27}–C_{30} alkenes in the air masses of the Arctic Ocean from Tromsø to Svalbard in the Summer ARctic Expedition (AREX) (Ferrero et al., 2019). Therefore, it indicates that the *n*-alkanes may introduced from the atmospheric sources accumulated in the snow and tidewater glacier. Moreover, in a previous study, homologous series of n-alkanes from C22 to C33 were identified in the soil and marine sediment around the Kongsfjorden (Kim et al., 2011). They reported that the average $CPI_{C25–C31}$ values for soil and sediment were 12.6 ± 6.5 (n = 15) and 1.4 ± 0.3 (n = 29), respectively. Moreover, the ACLs in soil and sediment were 29.0 ± 0.8 (n = 15) and 28.1 ± 0.2 (n = 29), respectively. This is distinguished from the $CPI_{C17–C35}$ (0.97 ± 0.11, n = 8) and ACL (24.6 ± 3.7, n = 8) of the surface layer in this study. It means that the *n*-alkane composition of surface seawater in this study reflects the influence of the snow and glacier rather than the soil, which is also the terrestrial source. Therefore, the *n*-alkane composition may have potential as a specific indicator for the influx of freshwater by tidewater glaciers and snow melting in the fjord system. In addition, these indicators will help evaluate the influence of the amounts of inflowing particulate and dissolved OM on the melting of tidewater glaciers.

4.3. Changes in marine environment with tidewater glacial melting

The measured POC flux in Kongsfjorden peaked when glaciers and sea ice melted in the spring when the total mass flux increased (D'Angelo et al., 2018). This suggests that organic carbon originating from glaciers plays an important role in this season. In addition, in a previous report, the enriched $\delta^{13}C$ (abnormal trend due to soil-derived bound inorganic nitrogen) and high C/N ratios identified in the surface sediments indicated that terrestrial OM is a major carbon source in the inner fjord, while a mixture of marine-terrestrial signals appeared in the outer fjord (Kim et al., 2011; Kumar et al., 2016). Higher organic carbon contents of the sediments were found in the outer fjord than in the inner region (Koziorowska et al., 2017; Kumar et al., 2016). Moreover, the results of an analysis of the concentrations of inorganic carbon in fjord sediments revealed that biogenic carbon predominates in the outer bays and that carbonates in the glacier front originate from terrestrial sources by tidewater glaciers (e.g., Forwick et al., 2010; Koziorowska et al., 2017). Recently, in future circulation predictions conducted using the Regional Ocean Modeling System (ROMS), the length of Kongsfjorden is predicted to increase from 27 km to 39 km, and the total area is also predicted to increase from 227 km^2 to 286 km^2 due to the retreat of tidal glaciers (Torsvik et al., 2019). Torsvik et al. (2019) also predicted that as the residence time of particles in the water column increases from an average of 10.7 days–12.9 days in the Ny-Ålesund to Blomstrandhalvøya transect, the supply of terrestrial OM provided by the internal circulation of Kongsfjorden will increase in importance as an OM source.

Based on the environmental conditions of Kongsfjorden, the following hypothesis can be proposed by considering the results of this study. The retreat of tidewater glaciers due to climate change occurring in the high Arctic fjord during the melting season could lead to the enhancement of the organic and inorganic carbon fluxes, the enhancement of the internal circulation of organic carbon and the increase of the sedimentation rate in the inner fjord. Even if the area of drift ice covering the sea surface decreases, the light will be blocked as the glaciers melt and the particle concentrations increase. Thus, it seems that rather a share of autochthonous OM will decrease, and the carbon cycle in fjords will change dramatically. In particular, the strong influence on phytoplankton and zooplankton caused by marine environmental changes will allow the regional ecosystem to be more clearly distinguished between the inner and outer fjord regions. Furthermore, these changes could be accelerated in fjord systems that are very susceptible to climate change.

5. Conclusions

In this study, we investigated the spatial distributions of organic compounds (sterols and *n*-alkanes) in the seawater of the high Arctic fjord system Kongsfjorden in Svalbard. The phytoplankton cell density spatially distinguished between the inner and outer fjord sites. Moreover, the distribution of the lipid biomarkers indicated that particulate OM derived from allochthonous sources was predominant in the inner fjord, while autochthonous sources were predominant in the outer fjord. The db-RDA results indicated that the major controlling factors for the distribution of organic compounds were the density and POC, including chl. *a*, concentrations in the study area. Notably, the concentration of short-chain alkenes was significantly high in the surface layer, suggesting the possibility of the use of these compounds as indicators for tidewater glaciers and snow melting. Consequently, the lipid biomarker approach could provide hints on the behavior and influence of POC in glaciers and the snow melting in Arctic fjord systems.

Funding

This research was a part of the project entitled "Carbon assimilation rate of sea ice ecosystem in the Kongsfjorden MIZ, Arctic (KOPRI, PE19170)". This work was also supported by the project titled 'Korea-Arctic Ocean Warming and Response of Ecosystem (K-AWARE, KOPRI, 1525011760)', funded by the Ministry of Oceans and Fisheries, Korea. And, the first author was partially supported by the Korea Polar Research Institute (KOPRI, PE21110).

Credit author statement

Jong-Ku Gal: original draft preparation, visualization. **Jong-Ku Gal, Bo Kyung Kim and Hyoung Min Joo**: conceptualization, and editing. **Hyoung Min Joo and Chorom Shim**: investigation of phytoplankton. **Jong-Ku Gal and Boyeon Lee**: investigation of biomarkers. **Il-Nam Kim and Jinyoung Jung**: supporting data, review and validation. **Kyung-Hoon Shin and Sun-Yong Ha**: supervision, review and funding acquisition.

Data availability statement

The data used in the figures will available in the Korea Polar Data Center (KPDC, https://kpdc.kopri.re.kr, https://dx.doi.org/doi:10.22663/KOPRI-KPDC-00001707.1).

Declaration of competing interest

The authors declare that they have no known competing financial interests or personal relationships that could have appeared to influence the work reported in this paper.

Acknowledgements

We appreciate the contributions of field members to the sample collection, and the careful support of the captain of the R/V Teisten. We also thank the Marine Laboratory in Ny-Ålesund for providing space and equipment for our research.

Appendix A. Supplementary data

Supplementary data to this article can be found online at https://doi.org/10.1016/j.envres.2021.112469.

References

Alley, R.B., Cuffey, K.M., Evenson, E.B., Strasser, J.C., Lawson, D.E., Larson, G.J., 1997. How glaciers entrain and transport basal sediment: physical constraints. Quat. Sci. Rev. 16, 1017–1038.

Boon, J.J., Rijpstra, W.I.C., de Lange, F., de Leeuw, J.W., Yoshioka, M., Shimizu, Y., 1979. Black sea sterol- a molecular fossil for dinoflagellate blooms. Nature. https://doi.org/10.1038/277125a0.

Box, J.E., Colgan, W.T., Christensen, T.R., Schmidt, N.M., Lund, M., Parmentier, F.J.W., Brown, R., Bhatt, U.S., Euskirchen, E.S., Romanovsky, V.E., Walsh, J.E., Overland, J. E., Wang, M., Corell, R.W., Meier, W.N., Wouters, B., Mernild, S., Mård, J., Pawlak, J., Olsen, M.S., 2019. Key indicators of Arctic climate change: 1971-2017. Environ. Res. Lett. 14.

Brassell, S.C., Eglinton, G., 1980. Environmental chemistry - an interdisciplinary subject. Natural and pollutant organic compounds in contemporary aquatic environments. In: Analytical Techniques in Environmental Chemistry. Pergamon Press, Oxford, pp. 1–22.

Brassell, S.C., Eglinton, G., Maxwell, J.R., Philp, R.P., 1978. Natural background of alkanes in the aquatic environment. In: Aquatic Pollutants. Pergamon Press, Oxford, pp. 69–86.

Bray, E.E., Evans, E.D., 1961. Distribution of n-paraffins as a clue to recognition of source beds. Geochem. Cosmochim. Acta 22, 2–15.

Brogi, S.R., Jung, J.Y., Ha, S.Y., Hur, J., 2019. Seasonal differences in dissolved organic matter properties and sources in an Arctic fjord: implications for future conditions. Sci. Total Environ. 694, 133740.

Bush, R.T., McInerney, F.A., 2013. Leaf wax n-alkane distributions in and across modern plants: implications for paleoecology and chemotaxonomy. Geochem. Cosmochim. Acta 117, 161–179. https://doi.org/10.1016/j.gca.2013.04.016.

Cecinato, A., Mabilia, R., Marino, F., 2000. Relevant organic components in ambient particulate matter collected at Svalbard Islands (Norway). Atmos. Environ. 34, 5061–5066.

Choi, H., Ha, S.Y., Lee, S., Kim, J.H., Shin, K.H., 2020. Trophic dynamics of zooplankton before and after polar night in the Kongsfjorden (Svalbard): evidence of trophic

position estimated by δ15N analysis of amino acids. Front. Mar. Sci. 7 https://doi.org/10.3389/fmars.2020.00489.
Cranwell, P.A., Eglinton, G., Robinson, N., 1987. Lipids of aquatic organisms as potential contributors to lacustrine sediments—II. Org. Geochem. 11, 513–527.
D'Angelo, A., Giglio, F., Miserocchi, S., Sanchez-Vidal, A., Aliani, S., Tesi, T., Viola, A., Mazzola, M., Langone, L., 2018. Multi-year particle fluxes in Kongsfjorden, Svalbard. Biogeosciences 15, 5343–5363.
Eglinton, G., Gonzalez, A.G., Hamilton, R.J., Raphael, R.A., 1962. Hydrocarbon constituents of the wax coatings of plant leaves: a taxonomic survey. Phytochemistry 1, 89–102.
Eglinton, G., Hamilton, R.J., 1967. Leaf epicuticular waxes. Science 156, 1322–1335. https://doi.org/10.1126/science.156.3780.1322.
Ferrero, L., Sangiorgi, G., Perrone, M., Rizzi, C., Cataldi, M., Markuszewski, P., Pakszys, P., Makuch, P., Petelski, T., Becagli, S., Traversi, R., Bolzacchini, E., Zielinski, T., 2019. Chemical composition of aerosol over the arctic ocean from summer arctic expedition (AREX) 2011–2012 cruises: ions, amines, elemental carbon, organic matter, polycyclic aromatic hydrocarbons, n-alkanes, metals, and rare earth elements. Atmosphere 10, 2011–2012.
Forwick, M., Vorren, T.O., Hald, M., Korsun, S., Roh, Y., Vogt, C., Yoo, K.C., 2010. Spatial and temporal influence of glaciers and rivers on the sedimentary environment in Sassenfjorden and Tempelfjorden. Spitsbergen. Geol. Soc. Lond. Spec. Publ. 344, 163–193.
Gal, J.K., Kim, J.H., Kim, D., Kang, S., Shin, K.H., 2018a. Assessing the saponification effect on the quantification of long chain alkenones and the $U^{K'}_{37}$ paleothermometer. Geochem. J. 52, 497–507.
Gal, J.K., Kim, J.H., Shin, K.H., 2018b. Distribution of long chain alkyl diols along a south-north transect of the northwestern Pacific region: insights into a paleo sea surface nutrient proxy. Org. Geochem. 119, 80–90.
Halbach, L., Vihtakari, M., Duarte, P., Everett, A., Granskog, M.A., Hop, H., Kauko, H.M., Kristiansen, S., Myhre, P.I., Pavlov, A.K., Pramanik, A., Tatarek, A., Torsvik, T., Wiktor, J.M., Wold, A., Wulff, A., Steen, H., Assmy, P., 2019. Tidewater glaciers and bedrock characteristics control the phytoplankton growth environment in a fjord in the Arctic. Front. Mar. Sci. 6, 1–8.
Han, D., Richter-Heitmann, T., Kim, I.N., Choy, E., Park, K.T., Unno, T., Kim, J., Nam, S. I., 2020. Survey of bacterial phylogenetic diversity during the glacier melting season in an Arctic fjord. Microb. Ecol. 81, 1–13.
Han, J., Calvin, M., 1969. Hydrocarbon distribution of algae and bacteria, and microbiological activity in sediments. Proc. Natl. Acad. Sci. U. S. A 64, 436–443.
Hood, E., Fellman, J., Spencer, R.G.M., Hernes, P.J., Edwards, R., Damore, D., Scott, D., 2009. Glaciers as a source of ancient and labile organic matter to the marine environment. Nature 462, 1044–1047.
Hopwood, M.J., Carroll, D., Dunse, T., Hodson, A., Holding, J.M., Iriarte, J.L., Ribeiro, S., Achterberg, E.P., Cantoni, C., Carlson, D.F., Chierici, M., Clarke, J.S., Cozzi, S., Fransson, A., Juul-Pedersen, T., Winding, M.H.S., Meire, L., 2020. Review article: how does glacier discharge affect marine biogeochemistry and primary production in the Arctic? Cryosphere 14, 1347–1383.
Hörner, T., Stein, R., Fahl, K., Birgel, D., 2016. Post-glacial variability of sea ice cover, river run-off and biological production in the western Laptev Sea (Arctic Ocean) – a high-resolution biomarker study. Quat. Sci. Rev. 143, 133–149.
Huang, W.-Y., Meinschein, W.G., 1976. Sterols as source indicators of organic materials in sediments. Geochem. Cosmochim. Acta 40, 323–330. https://doi.org/10.1016/0016-7037(76)90210-6.
Iversen, K.R., Seuthe, L., 2011. Seasonal microbial processes in a high-latitude fjord (Kongsfjorden, Svalbard): I. Heterotrophic bacteria, picoplankton and nanoflagellates. Polar Biol. 34, 731–749.
Jung, J., Hong, S.B., Chen, M., Hur, J., Jiao, L., Lee, Y., Park, K., Hahm, D., Choi, J.O., Yang, E.J., Park, J., Kim, T.W., Lee, S., 2020. Characteristics of methanesulfonic acid, non-sea-salt sulfate and organic carbon aerosols over the Amundsen Sea, Antarctica. Atmos. Chem. Phys. 20, 5405–5424.
Kang, S.H., Fryxell, G., Roelke, D.L., 1993. Fragilariopsis cylindrus compared with other species of the diatom family Bacillariaceae in Antarctic marginal ice-edge zones. In: Sims, P.A. (Ed.), Progress in Diatom Studies: Contributions to Taxonomy, Ecology and Nomenclature. Nova Hedwigia, pp. 335–352.
Kim, B.K., Joo, H.M., Jung, J., Lee, B., Ha, S.Y., 2020. In situ rates of carbon and nitrogen uptake by phytoplankton and the contribution of picophytoplankton in Kongsfjorden. Svalbard. Water 12, 2903.
Kim, J.H., Lee, D.H., Yoon, S.H., Jeong, K.S., Choi, B., Shin, K.H., 2017. Contribution of petroleum-derived organic carbon to sedimentary organic carbon pool in the eastern Yellow Sea (the northwestern Pacific). Chemosphere 168, 1389–1399.
Kim, J.H., Peterse, F., Willmott, V., Klitgaard Kristensen, D., Baas, M., Schouten, S., Sinninghe Damstéa, J.S., 2011. Large ancient organic matter contributions to Arctic marine sediments (Svalbard). Limnol. Oceanogr. 56, 1463–1474. https://doi.org/10.4319/lo.2011.56.4.1463.
Koziorowska, K., Kuliński, K., Pempkowiak, J., 2017. Distribution and origin of inorganic and organic carbon in the sediments of Kongsfjorden, Northwest Spitsbergen, European Arctic. Continent. Shelf Res. 150, 27–35.
Kuliński, K., Kędra, M., Legeżyńska, J., Gluchowska, M., Zaborska, A., 2014. Particulate organic matter sinks and sources in high Arctic fjord. J. Mar. Syst. 139, 27–37.
Kumar, V., Tiwari, M., Nagoji, S., Tripathi, S., 2016. Evidence of anomalously low δ13C of marine organic matter in an Arctic fjord. Sci. Rep. 6, 1–9.
Lawson, E.C., Wadham, J.L., Tranter, M., Stibal, M., Lis, G.P., Butler, C.E.H., Laybourn-Parry, J., Nienow, P., Chandler, D., Dewsbury, P., 2014. Greenland ice sheet exports labile organic carbon to the Arctic oceans. Biogeosciences 11, 4015–4028.
Marzi, R., Torkelson, B.E., Olson, R.K., 1993. A revised carbon preference index. Org. Geochem. 20, 1303–1306. https://doi.org/10.1016/0146-6380(93)90016-5.
Matsuda, H., Koyama, T., 1977. Early diagenesis of fatty acids in lacustrine sediments-II. A statistical approach to changes in fatty acid composition from recent sediments and some source materials. Geochem. Cosmochim. Acta 41, 1825–1834. https://doi.org/10.1016/0016-7037(77)90214-9.
McGovern, M., Pavlov, A.K., Deininger, A., Granskog, M.A., Leu, E., Søreide, J.E., Poste, A.E., 2020. Terrestrial inputs drive seasonality in organic matter and nutrient biogeochemistry in a high Arctic fjord system (Isfjorden, Svalbard). Front. Mar. Sci. 7, 1–15. https://doi.org/10.3389/fmars.2020.542563.
Moon, H.W., Wan Hussin, W.M.R., Kim, H.C., Ahn, I.Y., 2015. The impacts of climate change on Antarctic nearshore mega-epifaunal benthic assemblages in a glacial fjord on King George Island: responses and implications. Ecol. Indicat. 57, 280–292.
Parsons, P.R., Maita, Y., Lalli, C.M., 1984. A Manual of Chemical and Biological Methods for Seawater Analysis. Pergamon Press, Oxford.
Poynter, J., Eglinton, G., 1990. Molecular composition of three sediments from hole 717C: the Bengal Fan. In: Cochran, J.R., Curray, J.R., Sager, W.W., Stow, D.A.V. (Eds.), Proceedings of the Ocean Drilling Program, Scientific Results. Ocean Drilling Program, College Station, TX, pp. 155–161.
Pramanik, A., Van Pelt, W., Kohler, J., Schuler, T.V., 2018. Simulating climatic mass balance, seasonal snow development and associated freshwater runoff in the Kongsfjord basin, Svalbard (1980–2016). J. Glaciol. 64, 943–956.
Randers, J., Goluke, U., 2020. An earth system model shows self-sustained melting of permafrost even if all man-made GHG emissions stop in 2020. Sci. Rep. 10, 1–9.
R Development Core Team, 2015. R Core Team. R: A Language and Environment for Statistical Computing. R Foundation for Statistical Computing, Vienna, Austria.
Round, F.E., Crawford, R.M., Mann, D.G., 1990. The Diatom; Biology & Morfology of the Genera. Cambridge University Press, Great Britain.
Rontani, J.F., Belt, S.T., Amiraux, R., 2018. Biotic and abiotic degradation of the sea ice diatom biomarker IP25 and selected algal sterols in near-surface Arctic sediments. Org. Geochem. 118, 73–88. https://doi.org/10.1016/j.orggeochem.2018.01.003.
Schellenberger, T., Dunse, T., Kääb, A., Kohler, J., Reijmer, C.H., 2015. Surface speed and frontal ablation of Kronebreen and Kongsbreen, NW Svalbard, from SAR offset tracking. Cryosphere 9, 2339–2355. https://doi.org/10.5194/tc-9-2339-2015.
Smith, H.J., Foster, R.A., McKnight, D.M., Lisle, J.T., Littmann, S., Kuypers, M.M.M., Foreman, C.M., 2017. Microbial formation of labile organic carbon in Antarctic glacial environments. Nat. Geosci. 10, 356–359.
Stein, R., Grobe, H., Wahsner, M., 1994. Organic carbon, carbonate, and clay mineral distributions in eastern central Arctic ocean surface sediments. Mar. Geol. 119, 269–285.
Syvitski, J.P., Morehead, M.D., Nicholson, M., 1998. HYDROTREND: a climate-driven hydrologic-transport model for predicting discharge and sediment load to lakes or oceans. Comput. Geosci. 24, 51–68.
Syvitski, J.P.M., Peckham, S.D., Hilberman, R., Mulder, T., 2003. Predicting the terrestrial flux of sediment to the global ocean: a planetary perspective. Sediment. Geol. 162, 5–24.
Tomas, C.R., 1997. Identifying Marine Phytoplankton. Academic Press, San Diego, CA, USA.
Torsvik, T., Albretsen, J., Sundfjord, A., Kohler, J., Sandvik, A.D., Skarðhamar, J., Lindbäck, K., Everett, A., 2019. Impact of tidewater glacier retreat on the fjord system: modeling present and future circulation in Kongsfjorden. Svalbard. Estuar. Coast. Shelf Sci. 220, 152–165.
Vieli, A., Jania, J., Kolondra, L., 2002. The retreat of a tidewater glacier: observations and model calculations on Hansbreen, Spitsbergen. J. Glaciol. 48, 592–600.
Volkman, J.K., 1986. A review of sterol markers for marine and terrigenous organic matter. Org. Geochem. 9, 83–99.
Volkman, J.K., Barrett, S.M., Blackburn, S.I., Mansour, M.P., Sikes, E.L., Gelin, F., 1998. Microalgal biomarkers: a review of recent research developments. Org. Geochem. 29, 1163–1179.
Wang, Z., Fingas, M., Page, D.S., 1999. Oil spill identification. J. Chromatogr., A 843, 369–411.
Yunker, M.B., Macdonald, R.W., Veltkamp, D.J., Cretney, W.J., 1995. Terrestrial and marine biomarkers in a seasonally ice-covered Arctic estuary — integration of multivariate and biomarker approaches. Mar. Chem. 49, 1–50.